

**Density-driven spontaneous streak segregation patterns in a thin rotating drum**

C. C. Liao, S. S. Hsiau,\* and H. C. Nien

*Department of Mechanical Engineering, National Central University, No. 300, Zhongda Road, Zhongli 32001, Taiwan, Republic of China*

(Received 12 December 2013; published 13 June 2014)

Granular mixtures may segregate because of external driving forces, which play an important role in industry and geophysics. We investigate experimentally the mechanism of density-driven spontaneous streak segregation patterns in a thin rotating drum. We find that a spontaneous streak segregation pattern can occur in such a system, which we call a *D*-system. A phase diagram identifies three segregation pattern regimes in this study: the mixing regime, the core segregation regime, and the streak segregation regime.

DOI: [10.1103/PhysRevE.89.062204](https://doi.org/10.1103/PhysRevE.89.062204)

PACS number(s): 45.70.Mg, 45.70.Qj

**I. INTRODUCTION**

Granular materials and powders are collections of discrete solid particles dispersed in an interstitial fluid. Granular mixtures may segregate under external driving forces because of differences in size, density, or shape; such segregation can cause unpredictable problems in industrial processes, such as pharmaceutical products. Additionally, granular streak segregation patterns are an important issue in geophysics and are relevant to rock formation. It is accordingly important to understand the mechanism of granular segregation [1–20].

Two distinct regions are always observed in granular motions in a rotating drum with partially filled containers: a fixed bed region and a flowing layer region at the free surface where mixing and segregation of granular matter take place. Core segregation typically occurs in a binary mixture with different sizes or densities in a rotating drum due to percolation and buoyancy effects [1,19,20]. In addition, granular materials may segregate spontaneously in a regular streak segregation pattern. Previous studies have investigated the formation of size-induced streak segregation patterns [3,6–10]. The pattern formation is affected by many parameters such as rotation speed, fill level, and container geometry [7,8,14,15]. Makse *et al.* [3] reported that spontaneous streak segregation occurs when the large grains have a larger repose angle than the smaller grains. These authors also noted that stratification is related to the occurrence of avalanches. Gray and Hutter [6] experimentally studied pattern formation in granular avalanches with a binary mixture with different grain sizes. They found that during motion, the kinetic sieving of a bidispersed granular mixture creates a two-layer shear band in which the larger particles lie on top of the smaller particles. Hill *et al.* [7] studied radial segregation patterns in a size system in a thin rotating drum and found that the fill level has a significant effect on the radial segregation patterns. Zuriguel *et al.* [8] experimentally investigated granular segregation with different particle sizes in a thin rotating drum. Based on their measurements, they developed a simple model that predicts the number of streaks in the pattern. Zuriguel *et al.* also found that rotation speed, the size of the drum, and the volume fraction of small particles are important parameters for determining patterns. Meier *et al.* [9] reported that the radial streak pattern can become coarser in a thin rotating drum because of the

transport of small particles from streak to streak through the semicircular radial core. Hill *et al.* [14] indicated that the velocity field is coupled to the composition of the particles in the flowing layer. The flowing layer is thinner and moves faster when the flowing layer consists primarily of small particles. Conversely, a thicker and slower flowing layer is formed from larger particles.

Most previous studies have focused on core segregation; the mechanism behind spontaneous streak segregation patterns is less well understood. In particular, there have been no experimental studies of density-driven streak segregation patterns (*D*-systems). In this paper, we focus on the mechanism of density-driven spontaneous streak segregation patterns in a thin rotating drum. We systematically study the effects of density ratios and rotation speed on spontaneous streak segregation patterns. We show here that spontaneous streak segregation can be produced in a *D*-system. A phase diagram identifies three granular pattern regimes: a mixing regime, a core segregation regime, and a streak segregation regime.

**II. EXPERIMENTAL PROCEDURE**

We used a quasi-two-dimensional (2D) rotating drum with a diameter of 50 cm and a bed thickness of 0.9 cm to investigate density-driven spontaneous streak segregation. The front and back faceplates of the rotating drum were made of clear glass to permit optical access. Four kinds of beads, all with the same size ( $3 \pm 0.1$  mm in diameter) but different densities [stainless steel = 7.93 g/cm<sup>3</sup>, glass = 2.48 g/cm<sup>3</sup>, polyformaldehyde (POM) = 1.41 g/cm<sup>3</sup>, and polypropylene (PP) = 0.90 g/cm<sup>3</sup>], were used as the granular materials. The internal friction coefficients for the four kinds of materials used in this study were measured by using a commercial Jenike shearing tester. The values are 0.57 (stainless steel), 0.60 (glass), 0.58 (POM), and 0.62 (PP). Additionally, the restitution coefficients of the four materials used in this study, measured by the drop test, are 0.85 (stainless steel), 0.91 (glass), 0.90 (POM), and 0.92 (PP). The granular flows are dense in this study and the effect of the restitution coefficient on particle motions is less significant in dense granular flows. Moreover, surface friction effects on segregation in a rotating drum are still an open problem. Additionally, the differences in restitution and friction coefficients among the four granular materials are not significant. The dimensionless axial thickness of the drum, defined as the ratio of the drum axial length and the particle diameter, was set to 3 in this study. It is noted

\*Corresponding author: [sshsiau@cc.ncu.edu.tw](mailto:sshsiau@cc.ncu.edu.tw)

that effects of wall friction become significant when the axial length is too small. The axial motion may play a role as the axial thickness is increased. Therefore, a dimensionless axial thickness of 3 was chosen to balance the wall friction and axial motion. Six density ratios were used to investigate the density-driven streak segregation dynamic. The density ratios were  $\rho_h/\rho_l = 8.81$  (steel and PP), 5.62 (steel and POM), 3.20 (steel and glass), 2.76 (glass and PP), 1.76 (glass and POM), and 1.57 (POM and PP), where  $\rho_h$  is the density of the heavy particle and  $\rho_l$  is the density of the light particle in the binary mixture. The filling level of granular materials was fixed as 0.51. The volume fraction of the heavy and light beads was 50%-50% in each experimental test. Before each experiment, the binary mixture was well mixed. In this study, five rotation speeds were used to investigate density-induced spontaneous streak segregation patterns. In this study, we focus on the rolling regime where the flow is continuous. The experimental parameters used in the current experiments are listed in Table I. Because of observational difficulties, only the flows adjacent to the front faceplate could be recorded and analyzed. Before each experiment, the inner surface was cleaned and polished with wax to reduce wall friction effects. A digital camera (SONY HDR-SR8) was used to record the flow motions inside the drum at a speed of 30 frames per second (FPS) and a resolution of  $640 \times 480$  pixels. We defined a shape index to quantify the density-induced streak segregation [7]:

$$\text{shape index} \equiv \frac{p^2}{A}, \quad (1)$$

where  $p$  is the perimeter of the streak segregation pattern and  $A$  is the total area. The shape index becomes larger as the density-driven streak segregation becomes more defined and has more streaks. The segregation pattern may change from streak segregation to core segregation as the shape index decreases.

To investigate the density-induced spontaneous streak segregation mechanism, we measured the dynamic properties of the particles. Another high-speed camera (IDT MotionPro X3 PLUS) was used to record the motions of granular materials with 800 FPS near the center of the drum [shown in Fig. 4(b)] as the regular streak segregation pattern stabilizes. The particle tracking velocimetry technique was used to calculate the velocity of the beads by locating their centers in the high-speed images and determining their displacements between two consecutive images [4,21–23]. Figure 1 shows the image

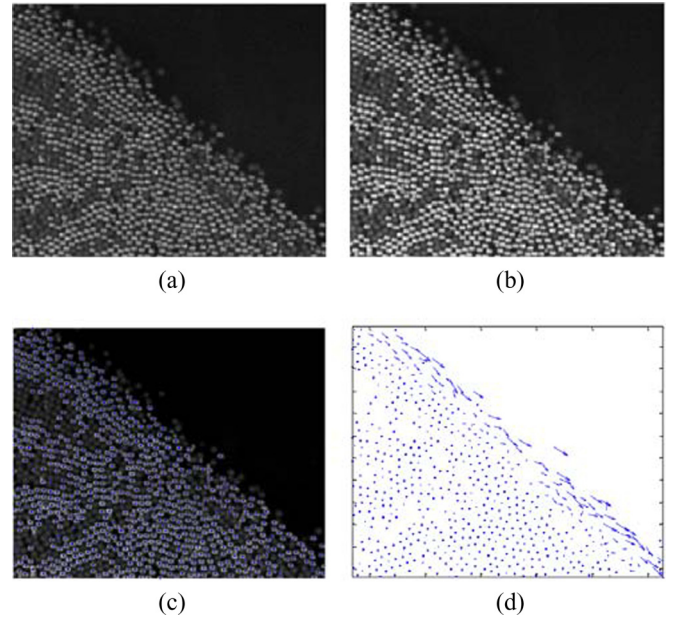


FIG. 1. (Color online) Image manipulation process: (a) the original gray-scale image, (b) the image after the Gaussian and Laplacian filtering process, (c) the image after locating the tracer particle, and (d) a typical flow field obtained from two consecutive images.

manipulation process used to obtain the velocity field in this study. The local ensemble average velocities  $\langle u \rangle$  (stream-wise direction) and  $\langle v \rangle$  (transverse direction) in each bin ( $3 \times 3 \text{ mm}^2$ ) were defined as follows:

$$\langle u \rangle = \frac{\sum_{k=1}^N u_k}{N}, \quad (2)$$

$$\langle v \rangle = \frac{\sum_{k=1}^N v_k}{N}, \quad (3)$$

where  $k$  represents the  $k$ th tracer particle,  $N$  is the total number of velocities used for averaging the mean values, and  $u_k$  and  $v_k$  are the instantaneous velocities of the  $k$ th tracer particle measured from a pair of consecutive images. The local fluctuation velocities in the two directions were calculated by

$$\langle u'^2 \rangle^{1/2} = \sqrt{\frac{\sum_{k=1}^N (u_k - \langle u \rangle)^2}{N}}, \quad (4)$$

$$\langle v'^2 \rangle^{1/2} = \sqrt{\frac{\sum_{k=1}^N (v_k - \langle v \rangle)^2}{N}}. \quad (5)$$

Ogawa [24] first introduced the concept of granular temperature to quantify the mean-square value of the fluctuation velocities. The granular temperature  $T$  was used to quantify the kinetic energy of granular flows and is a key property for studying the dynamic behavior of granular flows [21,22,24,25]. A granular system behaves more like a liquid or a gas when it has a relatively higher granular temperature. The local granular temperature in a quasi-2D system can be calculated from the

TABLE I. Experimental parameters used in the experiments.

Experimental particles configuration	Density ratio ( $\rho_h/\rho_l$ )	Rotation speed (rpm)
Steel & PP	8.81	
Steel & POM	5.62	0.6
Steel & Glass	3.20	0.8
		1.0
Glass & PP	2.76	1.2
Glass & POM	1.76	1.4
POM & PP	1.57	

fluctuation velocities of the particles:

$$T = \frac{\langle u^2 + v^2 \rangle}{2}. \tag{6}$$

The average spatial velocity and the average spatial granular temperature of heavy particles are calculated by averaging the corresponding values in the bins in the region near the center of the drum, as shown in Fig. 4(b). We note that only the velocities of the heavy particles and the granular temperature in the flowing layer are averaged to obtain the average spatial velocity and the average spatial granular temperature of heavy particles. We calculated the average depth of heavy particles by averaging all the positions of the tracer heavy particles in the transverse direction in the flowing layer in the region near the center of the drum.

**III. RESULTS AND DISCUSSION**

Figures 2(a)–2(f) show snapshots of the evolution of the system with a density ratio  $\rho_r = 2.76$  and  $\omega = 0.8$  rpm after

different numbers of revolutions. The heavy particles (glass beads) are marked in white and the light particles (PP beads) are marked in red. After half a revolution, a slight core segregation takes place, where the heavy particles sink to the bottom of the flowing layer and form the central core because of the buoyancy effect [Fig. 2(a)]. The start of the density-driven streak segregation pattern is seen after one revolution, as shown in Fig. 2(b). The streak segregation pattern becomes clearer after the streaks reenter the flowing layer and the stabilization of a regular streak pattern is reached after approximately three revolutions [Figs. 2(c)–2(f)]. In core segregation cases, the heavy particles sink to the lower part of the flowing layer and maintain lower velocities than the lighter particles [1]. However, the heavy particles may have larger velocities than the light particles in streak segregation cases since the binary mixture exhibits a larger difference in repose angle and density ratio. Therefore, the heavy particles can flow

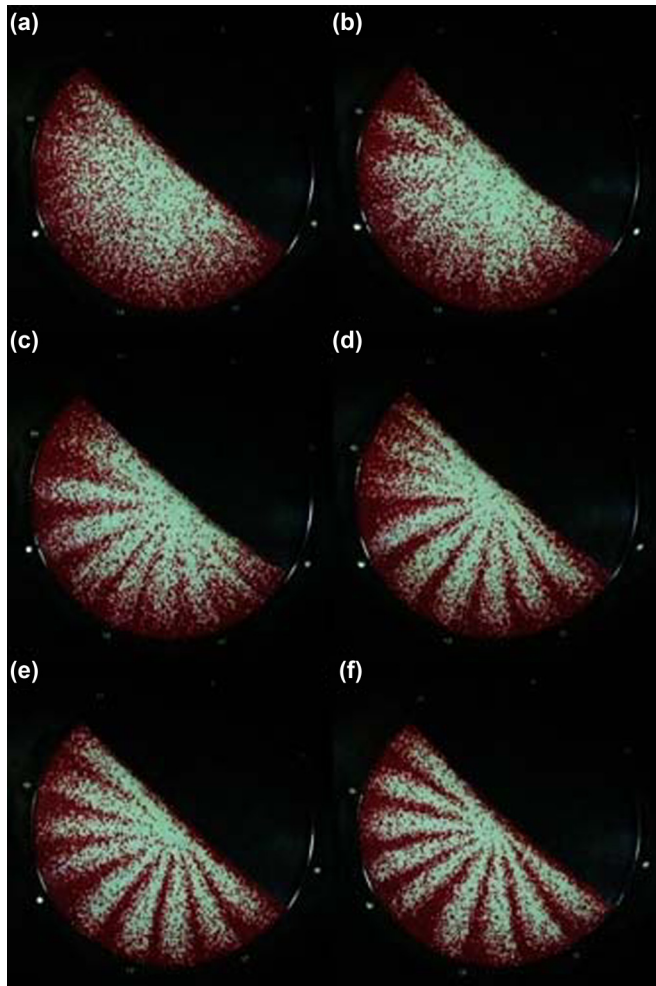


FIG. 2. (Color online) Snapshots of the drum at different revolutions for a density ratio  $\rho_r = 2.76$  and  $\omega = 0.8$  rpm. The white particles correspond to glass beads and the red particles correspond to PP beads. (a) 0.5 revolutions, (b) 1 revolution, (c) 1.5 revolutions, (d) 2 revolutions, (e) 2.5 revolutions, and (f) 3 revolutions.

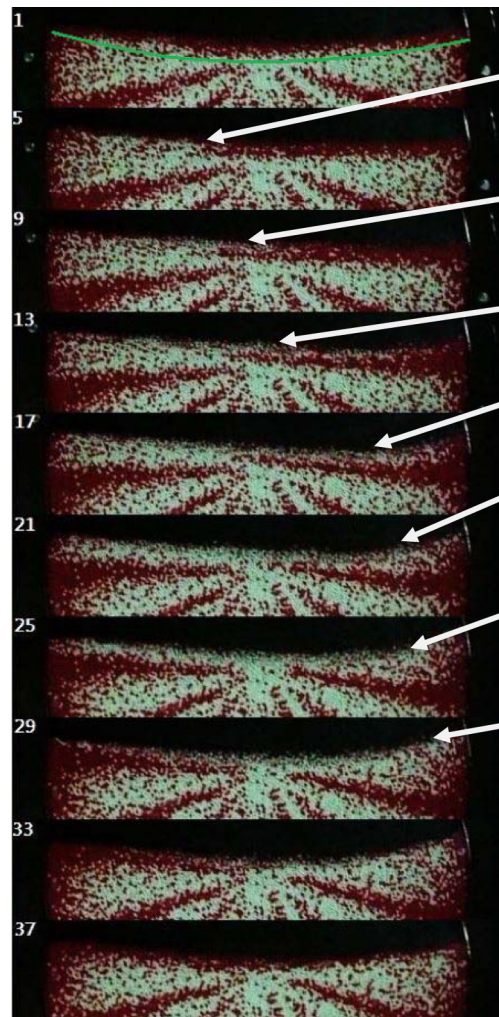


FIG. 3. (Color online) Snapshots captured from the imaged region after the density streak segregation pattern reached a steady state. The white particles correspond to glass beads and the red particles correspond to PP beads. The number that appears in each snapshot is the image sequence position for a camera with a grabbing speed of 10 FPS. The arrow indicates the process of the wave-breaking mechanism.

longer distances and create the streak segregation patterns shown in Fig. 2(b). As the undeveloped streak reenters the flowing layer, the heavy particles have more potential energy because the heavy particles are closer to the perimeter and move a longer distance, resulting in a clearer streak pattern [Fig. 2(c)]. After three revolutions, a regular streak pattern has stabilized, as shown in Fig. 2(f). Below, we discuss further the effect of the difference of repose angle and density ratio on radial segregation patterns.

Figure 3 shows snapshots after a regular streak pattern stabilizes, where the white particles correspond to glass beads and the red particles correspond to plastic beads (PP). The number listed in each snapshot is the image sequence

position, with a grabbing speed of 10 FPS. Hill *et al.* [12] first reported the mechanism of wave breaking to explain the streak segregation in *S*-systems. In this study, we use a wave-breaking mechanism to explain the density-induced spontaneous streak segregation mechanism in a *D*-system [12]. In streak segregation, the heavy white particles rise to the top surface of the flowing layer and cover the lighter red particles as the heavy particles move down. The arrows in Fig. 3 indicate the process of wave breaking occurring in the flowing layer and the curve in the uppermost image shows the approximate position of the flowing layer. When the streak enters the flowing layer and begins to flow down in the flowing layer, the velocities of the heavy particles (shown in white) are

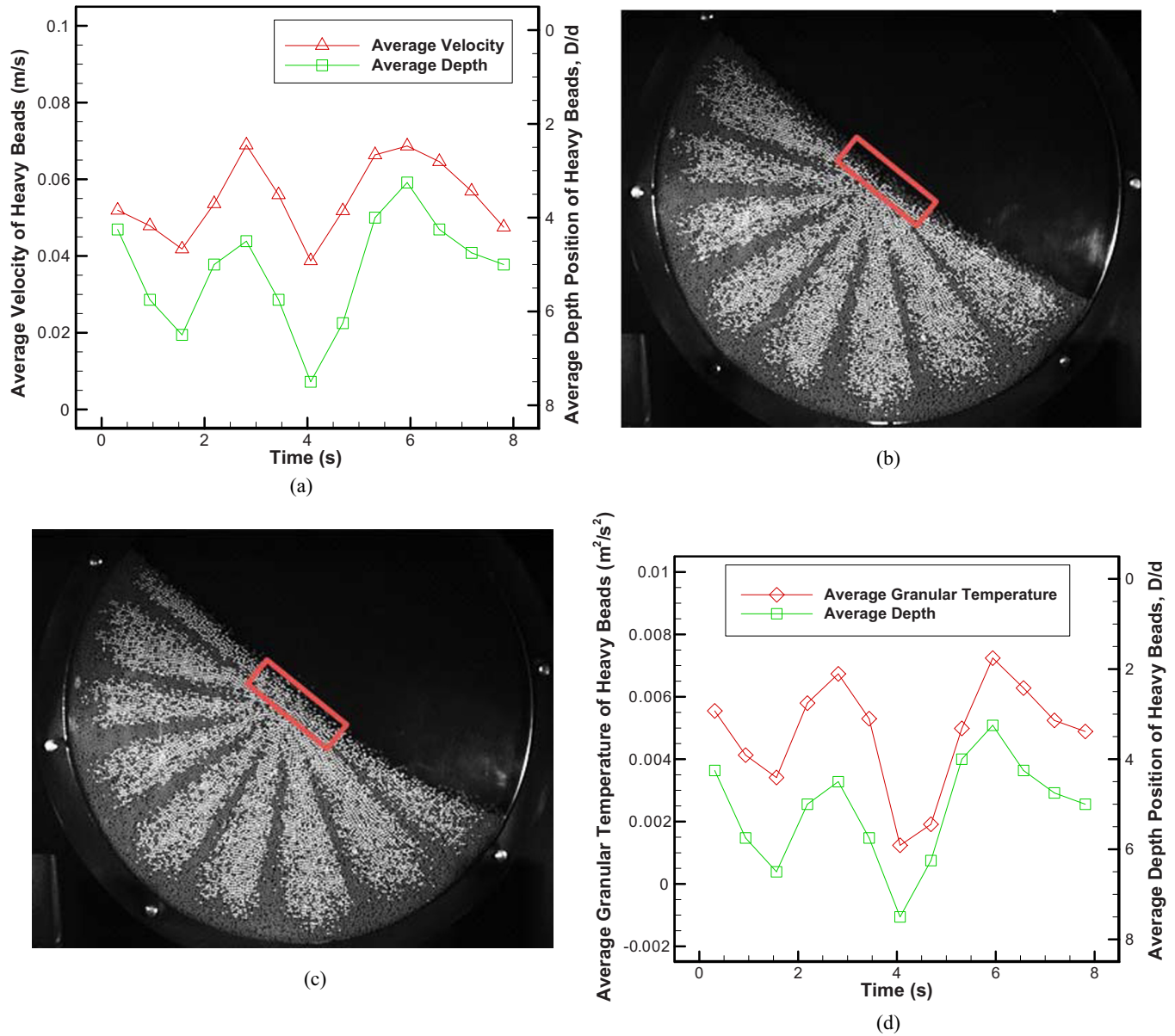


FIG. 4. (Color online) (a) Average velocity and average depth position of heavy particles plotted as a function of time, (b) a snapshot of the distribution of heavy particles in the observation zone after the flowing down of a streak, (c) a snapshot of the distribution of heavy particles in the observation zone during the process of a streak flowing down, and (d) the average granular temperature and average depth position of heavy particles plotted as a function of time, as the regular streak pattern stabilizes, with a density ratio  $\rho_r = 5.62$  and  $\omega = 1.0$  rpm.

larger than those of the lighter particles and the heavy particles flow over and cover the light particles, like the wave-breaking mechanism (Fig. 3).

Figure 4(a) shows the average velocity and average depth position of heavy particles plotted as a function of time as the regular streak pattern stabilizes, with a density ratio of  $\rho_r = 5.62$  and  $\omega = 1.0$  rpm. We note that each data point is averaged from 500 frames. The images were recorded after the regular streak pattern stabilized. Both average velocity and depth position in Fig. 4(a) were averaged from the two parameters of heavy particles in the bins in the rectangular cell [shown in Figs. 4(b) and 4(c)] in the flowing layer. It showed that the average velocity and average depth of heavy particles varied with time. The particle velocity in the flowing layer is dependent on the depth of the particles in the flowing layer. The particle velocity is larger near the free surface and smaller near the fixed bed. During the process of streaks flowing down in the flowing layer, the flowing layer contains mostly heavy particles, resulting in a smaller average depth and a larger average velocity of heavy particles. This finding is similar to results from a previous study [19]. Figures 4(b)–4(c) show snapshots of the distribution of heavy particles in the observation zone as the regular streak pattern stabilized. We observe that the flowing layer is predominantly composed of light particles after the streak flows down the flowing layer, as shown in Fig. 4(b). During the process of the streak flowing down, the heavy particles (shown in white) almost completely occupy the flowing layer because of the wave-breaking mechanism, as shown in Fig. 4(c). As a result, the heavy particles are located at a shallower average depth. These results are in agreement with the explanation given for the results shown in Fig. 4(a). Figure 4(d) shows the average granular temperature and average depth position of heavy particles plotted as a function of time as the regular streak pattern stabilizes. During the flowing down process of the streak pattern, the heavy particles were close to the free surface and had larger motions (larger fluctuation velocities and kinetic energy) and stronger collisions because of the higher velocity gradient, which led to the larger average granular temperature. This result is in agreement with the preceding statements.

Repose angle is an important parameter for investigating the granular flow behavior and has a significant influence on the flow dynamics of granular materials. In this study, we also measured the dynamic repose angle of monosized particles with various particle densities. The dynamic repose angle is determined while the drum is rotated through at least three revolutions to reach the stable flow field. Figure 5 shows the dynamic repose angle plotted as a function of rotation speed for the four materials used in this study. This figure shows that the dynamic repose angle increases with rotation speed. The dynamic repose angle is reduced for heavier particles because of the effects of gravity. Figure 6(a) shows the shape index plotted as a function of the number of revolutions for several rotation speeds for a density ratio  $\rho_r = 2.76$ . The shape index increases gradually with time and reaches a steady state in each case. More revolutions were required to reach the final stable shape index with increasing rotation speed. The segregation mechanism only occurred in the flowing layer. The particle velocity was enhanced and the resident time in the flowing layer was reduced as the rotation speed was increased.

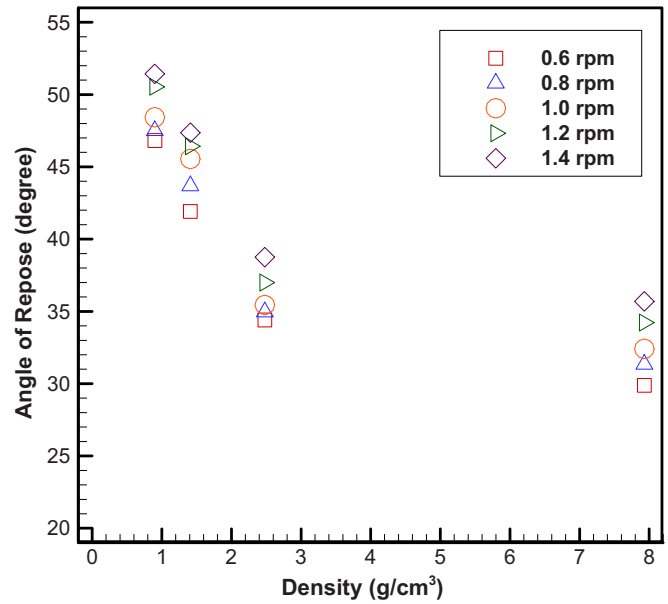


FIG. 5. (Color online) Dynamic repose angle of monosized particles plotted as a function of particle density for various rotation speeds.

As a result, a larger number of revolutions was required to reach the regular streak segregation pattern. Figure 6(b) shows the number of streaks in a final stable pattern plotted as a function of rotation speed. The number of streak segregations decreased with increasing rotation speed for each density ratio. This figure reveals that the number of final stable streak segregations increased for smaller density ratios. The flowing layer thickness becomes thicker for a higher rotation speed. As a result, more heavy particles are in the flowing layer, which results in a larger and thicker streak with increasing rotation speed. This result is similar to the findings of previous studies by Zuriguel *et al.* [8,10], where these authors also found that the number of streaks is inversely proportional to the rotation speed. The equation of the frequency of the rotation is given by [8]

$$\lambda = \omega T, \tag{7}$$

where  $\lambda$  is the angular distance between two consecutive streaks,  $\omega$  is the rotation speed (rad/s), and  $T$  is the period of each passing streak. Furthermore,  $T$  should be different for each different density ratio based on Eq. (7). The dimensionless difference of dynamic repose angle  $(\theta_l - \theta_h)/\theta_l$ , where  $\theta_l$  is the dynamic repose angle of monosized light particles and  $\theta_h$  is the dynamic repose angle of monosized heavy particles, is plotted as a function of the passage time  $T$  in Fig. 6(c). This figure shows that the dimensionless difference in the dynamic repose angle increases linearly with the passage time of  $T$ . The largest difference in dynamic repose angle was measured for a density ratio  $\rho_r = 8.81$ . Therefore, the number of streak segregations was smaller in this instance than in the other cases.

Figure 7 shows the dimensionless difference of dynamic repose angle  $(\theta_l - \theta_h)/\theta_l$  plotted as a function of density ratio. From this phase diagram, we identify three regimes: a mixing zone regime, a core segregation regime, and a density-driven

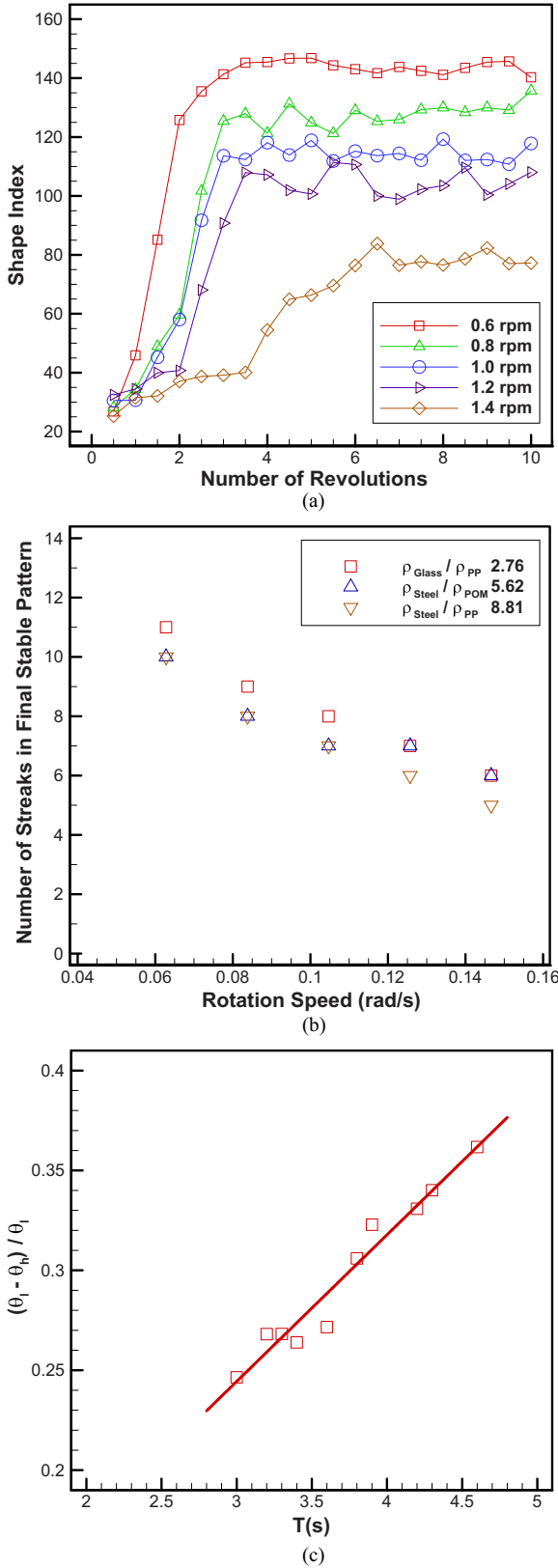


FIG. 6. (Color online) (a) Shape index plotted as a function of revolution number for different rotation speeds, at a density ratio  $\rho_r = 2.76$ , (b) the number of streak segregations in a final stable pattern plotted as a function of rotation speed, and (c) the dimensionless difference in dynamic repose angle  $(\theta_l - \theta_h) / \theta_l$  plotted as a function of the passage time  $T$ .

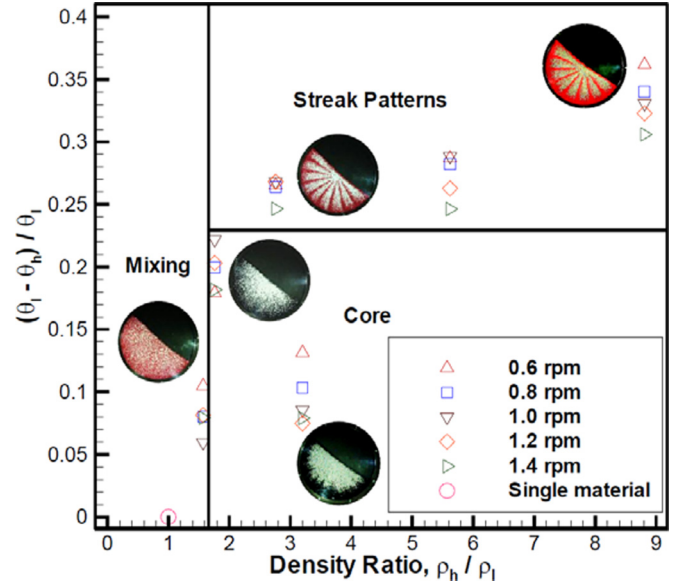


FIG. 7. (Color online) The dimensionless difference in dynamic repose angle  $(\theta_l - \theta_h) / \theta_l$ , plotted as a function of density ratio.

streak segregation regime. The circle highlighted in the mixing regime is the case of identical particles, where the density ratio is 1 and the difference in repose angle is 0. Therefore, segregation does not occur because there is no driving force. Additionally, segregation also does not occur with the case POM and PP (density ratio = 1.57) because of the small driving force of segregation (buoyancy effect). In the mixing regime, particle diffusion is the dominant mechanism to affect the granular pattern. The driving force of segregation (buoyancy effect) increases with the density ratio. The segregation occurs as the density ratio  $\geq 1.76$  with the sufficient driving force of segregation in this study. Additionally, core segregation occurs with the smaller difference in dynamic repose angle. According to the phase diagram, density-driven streak segregation occurs when there is a relatively large difference in dynamic repose angle and density ratio. The repose angle of mixture  $\theta_{\text{mix}}$  should be larger than  $\theta_h$  and smaller than  $\theta_l$  at the same rotation speed. This means that the heavy particles of mixture have larger repose angle and the greater potential energy with large difference in dynamic repose angle. Consequently, the heavy particles have larger velocity and inertia force as they flow down. As a result, the heavy particles can flow a long distance and form a streak segregation. The heavy particles cannot generate the sufficiently large velocity and inertia force as the difference in dynamic repose angle is not large enough. Therefore, the heavy particles easily sink to the bottom of the flowing layer due to the buoyancy effect and form the core segregation like the case of steel and glass with density ratio = 3.20.

#### IV. CONCLUSIONS

We report new experimental results of density-driven spontaneous streak segregation patterns in a thin rotating drum. We demonstrate the mechanism of spontaneous streak segregation patterns in  $D$ -systems. We find that the dimensionless

difference in dynamic repose angle and density ratio has a significant effect on the density-driven streak segregation patterns. The passage time of  $T$  increases linearly with the dimensionless difference in the dynamic repose angle. In this study, three different segregation regimes—a mixing zone regime, a core segregation regime, and a density streak segregation regime—can be predicted based on the phase diagram. The streak segregation patterns can occur only for larger dimensionless differences in the dynamic repose angle and density ratio. This study provides the experimental data

necessary for theoretical work, such as the development of a model to determine the spontaneous streak segregation in  $D$ -systems.

#### ACKNOWLEDGMENTS

The authors acknowledge support from the National Science Council of the Republic of China through Grant No. NSC 100-2221-E-008-078-MY3. We thank Professor M. L. Hunt for her helpful discussions.

- 
- [1] N. Jain, J. M. Ottino, and R. M. Lueptow, *Phys. Rev. E* **71**, 051301 (2005).
- [2] M. J. Woodhouse, A. R. Thornton, C. G. Johnson, B. P. Kokelaar, and J. M. N. T. Gray, *J. Fluid Mech.* **709**, 543 (2012).
- [3] H. A. Makse, S. Havlin, P. R. King, and H. E. Stanley, *Nature (London)* **386**, 379 (1997).
- [4] C. C. Liao, S. S. Hsiau, and K. To, *Phys. Rev. E* **82**, 010302(R) (2010).
- [5] C. C. Liao, S. S. Hsiau, T. H. Tsai, and C. H. Tai, *Chem. Eng. Sci.* **65**, 1109 (2010).
- [6] J. M. N. T. Gray and K. Hutter, *Continuum Mech. Thermodyn.* **9**, 341 (1997).
- [7] K. M. Hill, G. Gioia, and D. Amaravadi, *Phys. Rev. Lett.* **93**, 224301 (2004).
- [8] I. Zuriguel, J. M. N. T. Gray, J. Peixinho, and T. Mullin, *Phys. Rev. E* **73**, 061302 (2006).
- [9] S. W. Meier, D. A. M. Barreiro, J. M. Ottino, and R. M. Lueptow, *Nat. Phys.* **4**, 244 (2008).
- [10] I. Zuriguel, J. Peixinho, and T. Mullin, *Phys. Rev. E* **79**, 051303 (2009).
- [11] C.-C. Liao, S.-S. Hsiau, and C.-S. Wu, *Phys. Rev. E* **86**, 061316 (2012).
- [12] K. M. Hill, G. Gioia, D. Amaravadi, and C. Winter, *Complexity* **10**, 79 (2005).
- [13] G. G. Pereira, S. Pucilowski, K. Liffman, and P. W. Cleary, *Appl. Math. Modell.* **35**, 1638 (2011).
- [14] K. M. Hill, D. V. Khakhar, J. F. Gilchrist, J. J. McCarthy, and J. M. Ottino, *Proc. Natl. Acad. Sci. USA* **96**, 11701 (1999).
- [15] K. M. Hill, N. Jain, and J. M. Ottino, *Phys. Rev. E* **64**, 011302 (2001).
- [16] J. M. N. T. Gray and A. R. Thornton, *Proc. R. Soc. London, Ser. A* **461**, 1447 (2005).
- [17] A. R. Thornton, J. M. N. T. Gray, and A. J. Hogg, *J. Fluid Mech.* **550**, 1 (2006).
- [18] S. J. Fiedor and J. M. Ottino, *J. Fluid Mech.* **533**, 223 (2005).
- [19] N. Jain, J. M. Ottino, and R. M. Lueptow, *Granular Matter* **7**, 69 (2005).
- [20] D. V. Khakhar, J. J. McCarthy, and J. M. Ottino, *Phys. Fluids* **9**, 3600 (1997).
- [21] S. S. Hsiau and Y. H. Shieh, *J. Rheol.* **43**, 1049 (1999).
- [22] C. C. Liao, S. S. Hsiau, and W. J. Yu, *Int. J. Multiphase Flow* **46**, 22 (2012).
- [23] V. V. R. Natarajan, M. L. Hunt, and E. D. Taylor, *J. Fluid Mech.* **304**, 1 (1995).
- [24] S. Ogawa, in *Proceedings of US-Japan Seminar on Continuum-Mechanical and Statistical Approaches in the Mechanics of Granular Materials*, edited by S. C. Cowin and M. Satake (Gakujutsu Bunken Fukyu-kai, Tokyo, 1978), p. 208.
- [25] C. S. Campbell, *Annu. Rev. Fluid Mech.* **22**, 57 (1990).